Catalytic Hydrogenation

DOI: 10.1002/anie.200903620

Supramolecular Catalyst for Aldehyde Hydrogenation and Tandem Hydroformylation–Hydrogenation**

*Lisa Diab, Tomáš Šmejkal, Jens Geier, and Bernhard Breit**

In the past few years, many remarkable advances have been made in the emerging field of supramolecular catalysis. For example, large numbers of potential catalysts formed by self-assembly can now be varied in an expedient way by simply changing the constituent building blocks.[1] This development paves the way for the design of synthetic catalysts to mimic natural enzymes in substrate recognition and activation. Improved catalytic activity and selectivity should result, as well as the discovery of new synthetically useful transformations.[2]

The hydroformylation of alkenes is one of the major industrial processes currently carried out under homogeneous catalysis.[3] Nevertheless, aldehydes—the primary products of the hydroformylation—have virtually no importance as final products. Aldehydes are typically converted into alcohols, which find application as solvents and as raw materials for plasticizers and detergents. The hydrogenation is usually conducted in a separate step; however, alcohols can also be produced as tandem hydroformylation–hydrogenation products through the use of cobalt catalysts, albeit in lower yield and under harsh conditions.[4] Despite considerable efforts in this area, the final goal of chemo- and regioselective hydroformylation to give alcohol products under mild conditions remains elusive.[5] Ligand–metal bifunctional catalysis has recently become a valuable method for the hydrogenation of the C=O double bond. The key mechanistic step involves a unique concerted, outer-sphere reduction in which the substrate does not coordinate to the metal prior to the addition of dihydrogen.[6,7] We reasoned that the development of a novel hydrogenation catalyst based on a neutral rhodium hydride/phosphine complex (privileged hydroformylation catalyst) for hydroformylation under mild conditions would be the necessary first step toward an efficient tandem hydroformylation–hydrogenation.

In previous studies, we developed a supramolecular ligand system **1** (Scheme 1) that combines structural features of phosphine ligands (the metal-binding unit) with an acyl guanidinium functionality for the recognition of carboxylate groups.[2a] A rhodium catalyst based on this ligand was applied successfully in the highly regioselective hydroformylation of β,γ-unsaturated carboxylic acids[2a] and the decarboxylative hydroformylation of α,β-unsaturated carboxylic acids.[2b]

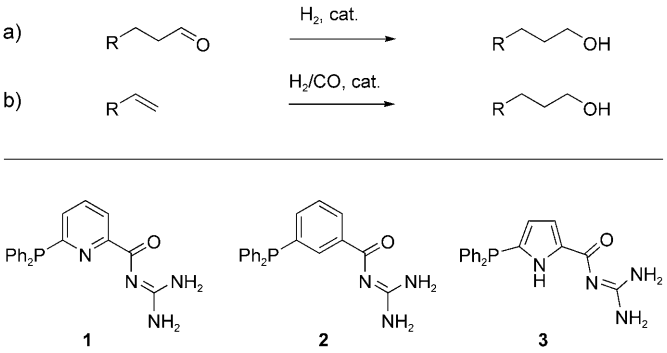

Scheme 1. a) Aldehyde hydrogenation, b) tandem hydroformylation–hydrogenation, and the structures of supramolecular ligands **1**–**3**.

We show herein that an appropriately designed phosphine ligand equipped with an acyl guanidine functionality can bind further substrates containing an electron-rich binding site (e.g. an aldehyde functionality) by hydrogen bonding, decrease the energy level of the lowest unoccupied molecular orbital (LUMO) of the substrate, and activate the substrate for a transition-metal-catalyzed reaction.[8,9] We designed a new ligand **3**, related to ligands **1** and **2**, with a pyrrole NH group as an additional hydrogen-donor functionality (Scheme 1). This modification was expected to result in a stronger interaction with generally weakly binding neutral host molecules.[10]

Ligand **3** was synthesized readily by coupling of the N-protected 5-diphenylphosphanylpyrrole-2-carboxylic acid **4** with mono-Boc-protected guanidine and subsequent deprotection catalyzed by trifluoroacetic acid (see the Supporting Information for details). The addition of sodium carbonate liberated the acyl guanidine (Scheme 2). Single crystals of **3** that were suitable for X-ray crystallography were grown from a saturated solution in ethyl acetate/pentane. X-ray crystal-structure analysis showed the formation of a hydrogen-bonded 1:1 adduct with ethyl acetate. The guanidinium functionality forms a twofold hydrogen bond to the ester carbonyl group (Figure 1).[11] This behavior may be viewed as a hint as to how this ligand is able to mediate carbonyl binding and activation.

We first examined the reaction of *n*-octanal (**5**) under standard hydroformylation conditions (CO/H_2, 20 bar). As

[*] Dr. L. Diab, Dr. T. Šmejkal, Dr. J. Geier, Prof. Dr. B. Breit
Institut für Organische Chemie und Biochemie
Freiburg Institute for Advanced Studies (FRIAS)
Albert-Ludwigs-Universität Freiburg
Alberstrasse 21, 79104 Freiburg (Germany)
Fax: (+49) 761-203-8715
E-mail: bernhard.breit@chemie.uni-freiburg.de
Homepage: http://portal.uni-freiburg.de/oc-breit

[**] This research was supported by the DFG, the International Research Training Group "Catalysts and Catalytic Reactions for Organic Synthesis" (IRTG 1038), the Fonds der Chemischen Industrie, BASF, and Wacker (donation of chemicals).

Supporting information for this article is available on the WWW under http://dx.doi.org/10.1002/anie.200903620.

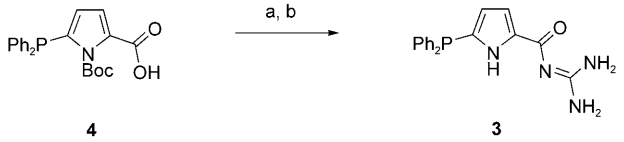

4 3

Scheme 2. Synthesis of ligand **3**: a) mono-Boc-guanidine, *N*-methylmorpholine, BOP, DMF, room temperature (77%); b) trifluoroacetic acid, room temperature, then Na_2CO_3, CH_2Cl_2 (56%). Boc = *tert*-butoxycarbonyl, BOP = benzotriazol-1-yloxytris(dimethylamino)phosphonium hexafluorophosphate, DMF = *N*,*N*-dimethylformamide.

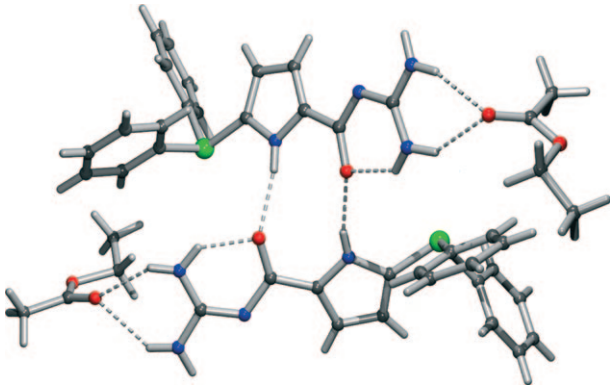

Figure 1. Crystal structure of ligand **3**. A disordered *n*-pentane molecule is omitted for clarity.

expected, no activity for the hydrogenation of the C=O functionality was observed when $[Rh(CO)_2(acac)]/PPh_3$ was used as a catalyst (Table 1, entry 1). Under the same conditions, the equivalent catalyst based on ligand **1** showed very low hydrogenation activity (3% conversion; Table 1, entry 2). However, a significant improvement was observed with ligands **2** and **3**. With these ligands, *n*-octanol was formed with 97 and 100% conversion, respectively (Table 1, entries 3 and 4).

Interestingly, the reaction became significantly slower when it was conducted under an atmosphere of pure hydrogen (Table 1, entry 5). This result suggests that the active hydrogenation catalyst has at least one CO ligand and is probably the typical trigonal-bipyramidal hydroformylation catalyst $[(R_3P)_2Rh(CO)_2H]$. The addition of small amounts of the strong acid CF_3SO_3H had a positive effect on the reaction rate (Table 1, compare entries 4 and 6). Acid promotes the formation of the guanidinium cation, which may be responsible for the interaction with the substrate (see below).

Having established the optimal reaction conditions, we focused on chemoselectivity and functional-group compatibility for the reduction of various substituted aldehydes. Aliphatic and aromatic aldehydes gave excellent results (Table 2, entries 1 and 2). Interestingly, remote nonconjugated internal double bonds in the substrate molecule were not affected at all (Table 2, entries 3 and 4). However, in the case of the α,β-unsaturated aldehyde oct-2-enal, we identified reaction conditions that enabled chemoselective reduction to furnish either the completely saturated alcohol or the aliphatic aldehyde, depending on the catalyst/substrate ratio and the substrate concentration (Scheme 3).

When a β-disubstituted α,β-unsaturated aldehyde and an α,β,γ,δ-unsaturated system were used as substrates with the Rh^I/**3** catalyst, only the corresponding α,β-unsaturated alcohols were formed; these alcohols were obtained in excellent yields (Table 2, entries 5 and 6). The equivalent triphenylphosphine/rhodium catalyst did not show any reactivity at all with α,β-unsaturated aldehydes under identical reaction conditions (see the Supporting Information). A wide range of functional groups, including ether, ester, and carbamate groups as well as a silyl ether, were found to be compatible with the optimized reaction conditions (Table 2, entries 7–10).

Table 1: Reduction of octanal.[a]

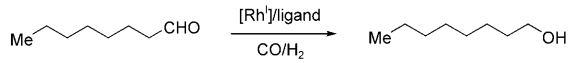

5 6

Entry	Ligand	Conversion [%]	Yield [%]
1	PPh_3	0	0
2	**1**	3	3
3	**2**	97	95
4	**3**	100	97
5[b]	**3**	27	27
6[c]	**3**	89	79

[a] Reaction conditions: $[Rh(CO)_2acac]$/ligand/substrate/CF_3SO_3H (1:10:500:5), CH_2Cl_2 (2 mL), c_0(**5**) = 0.6 M, CO/H_2 (1:1, 20 bar), 20 h, 40°C. Substrate conversion and yields were determined by GC. [b] The reaction was carried out under H_2 (20 bar), without CO. [c] The reaction was carried out without CF_3SO_3H. acac = acetylacetonate.

Table 2: Reduction of aldehydes.[a]

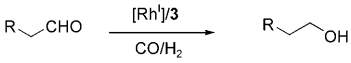

Entry	Product	Yield [%][c]
1	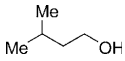	90
2[b]	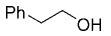	98
3	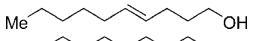	94
4	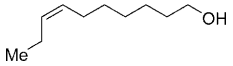	95
5	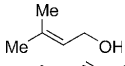	99
6[b]	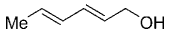	80
7	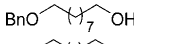	96
8	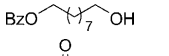	99
9	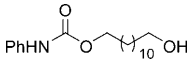	95
10	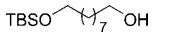	98
11	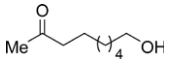	98

[a] Reaction conditions: $[Rh(CO)_2acac]$/**3**/substrate/CF_3SO_3H (1:10:500:5), c_0(substrate) = 0.6 M, CH_2Cl_2 (2 mL), CO/H_2 (1:1, 20 bar), 20 h, 40°C. Bn = benzyl, Bz = benzoyl, TBS = *tert*-butyldimethylsilyl. [b] $[Rh(CO)_2acac]$/**3**/substrate/CF_3SO_3H 1:10:100:5. [c] Yield of the isolated product.

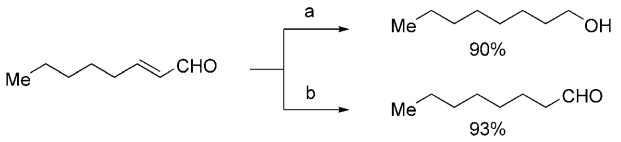

Scheme 3. Chemoselective reduction of oct-2-enal: a) $[Rh(CO)_2acac]$/**3**/substrate/CF_3SO_3H (1:10:500:5), c_0(substrate) = 0.6 M, CH_2Cl_2 (2 mL), CO/H_2 (1:1, 20 bar), 20 h, 40 °C; b) $[Rh(CO)_2acac]$/**3**/substrate/CF_3SO_3H (1:10:1000:5), c_0(substrate) = 0.2 M, CH_2Cl_2 (2 mL), CO/H_2 (1:1, 20 bar), 3 h, 40 °C. The yields were determined by GC.

Furthermore, the catalyst is completely selective for aldehyde reduction in the presence of a ketone functionality (Table 2, entry 11). In competition experiments between octanal and several ketones (acetophenone, benzophenone, ethyl acetoacetate, and trifluoroacetophenone), the aldehyde was hydrogenated with complete selectivity (see the Supporting Information).

We undertook a number of experiments to clarify the reaction mechanism. When methanol, which is known to disturb hydrogen bonding, was used as the solvent, a significant decrease in the activity of the catalyst was observed (Table 3, entry 2). No reaction was observed with

Table 3: Control experiments.[a]

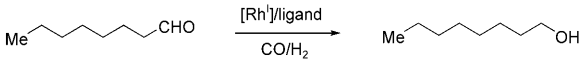

5 6

Entry	Ligand	Solvent	Yield [%]
1	**3**	CH_2Cl_2	97
2	**3**	MeOH	10
3	no ligand	CH_2Cl_2	0
4	PPh_3/**7**	CH_2Cl_2	0
5	**8**	CH_2Cl_2	10

[a] Reaction conditions: $[Rh(CO)_2acac]$/ligand/**5**/CF_3SO_3H (1:10:500:5), c_0(**5**) = 0.6 M, CH_2Cl_2 (2 mL), 40 °C, CO/H_2 (1:1, 20 bar), 20 h.

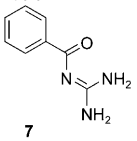

7

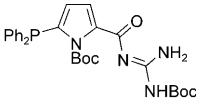

8

the unmodified rhodium complex $[Rh(CO)_2acac]$ (Table 3, entry 3) or when a combination of triphenylphosphine and the acyl guanidine additive **7** was used (Table 3, entry 4). The use of ligand **8**, which incorporates an *N*-Boc-protected guanidine moiety, furnished a slow catalyst (Table 3, entry 5). These results taken together provide strong evidence for an intramolecular reduction pathway that involves both the rhodium metal center and the guanidine functionality.

If this hydrogenation reaction occurs through a supramolecular mechanism, it should display saturation kinetics. Indeed, the hydrogenation of octanal at various substrate concentrations (0.05–0.6 M) revealed that the reaction kinetics obeys the Michaelis–Menten equation ($K_M = 0.1$ M and $V_{max} = 134\ h^{-1}$, $R^2 = 0.93$; see the Supporting Information for details).[12] Further, the supramolecular interaction of octanal with both the neutral and the protonated acyl guanidine ($K_{ass} = 30\ M^{-1}$, $CDCl_3$, 40 °C) was confirmed by ^1H NMR spectroscopy (see the Supporting Information for experimental details).

On the basis of the above results, we propose a mechanistic hypothesis for this hydrogenation reaction (Scheme 4). The mechanism involves coordination of the aldehyde to the

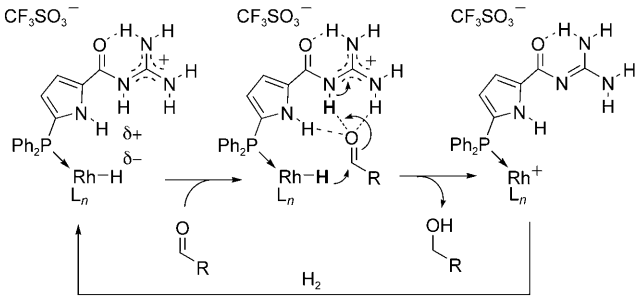

Scheme 4. Proposed mechanism for aldehyde hydrogenation catalyzed by [Rh]/**3**.

protonated guanidine moiety. This interaction may activate the aldehyde (decrease its LUMO energy;[13] see the Supporting Information) for the subsequent metal–ligand bifunctional hydrogenation. The catalyst is supposed to provide an acidic (from guanidine) and a hydridic hydrogen atom (at the rhodium center) in a concerted manner. In the next step, the basic guanidine functionality may facilitate the heterolytic cleavage of hydrogen and regeneration of the active catalyst.[14]

Further support for this mechanism came from DFT calculations,[15] which enabled the identification of a transition state for the hydride-transfer reaction (Figure 2). Thus, in the calculated catalyst–substrate complex, the aldehyde is bound to the guanidinium unit by two hydrogen bonds. Interestingly, on the way to the transition state, a third hydrogen bond to the pyrrole NH group develops. Finally, after proton and hydride transfer, the alcohol product is bound to one guanidine N atom and the pyrrole NH functionality. Hence, participation of the pyrrole NH group in the reaction mechanism may account for the observed efficiency of ligand **3** in the hydrogenation reaction.

With an efficient hydrogenation catalyst that operates under hydroformylation conditions in hand, we carried out first investigations of the proposed tandem hydroformylation–hydrogenation (Table 4). Terminal alkenes **9** (Table 4, entries 1–3) were converted into the corresponding alcohols with good regioselectivities (**10**/**11** up to 92:8) under mild conditions (40 °C, 40 bar). Interestingly, in the case of the methyl ketone functionalized alkene (Table 4, entry 3), the ketone was not touched at all under these reaction conditions. In the case of styrene, the branched alcohol was formed as the major regioisomer (Table 4, entry 4). This regiochemical outcome was also observed for the rhodium-catalyzed hydroformylation of aryl-substituted alkenes with a monodentate phosphine ligand.[16]

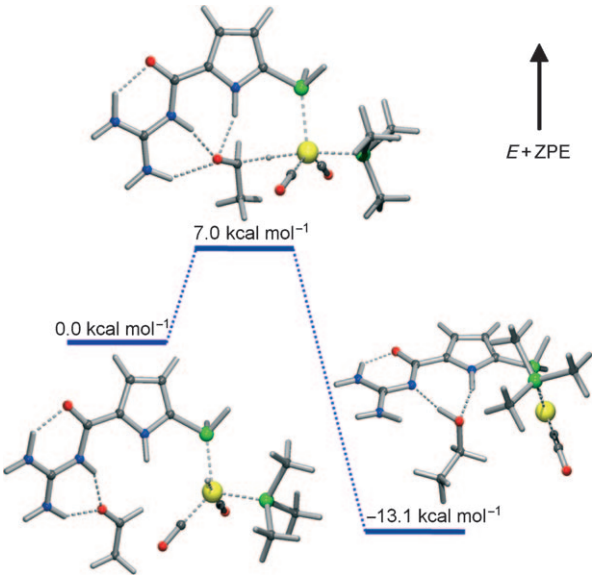

Figure 2. DFT calculations (B3LYP/6-31G-(d,p)[C,H,N,O,P] + LanL2DZ[Rh]) on the reaction mechanism and transition-state structure (E + ZPE = electronic energy + zero-point energy).

Table 4: Tandem hydroformylation–hydrogenation.[a]

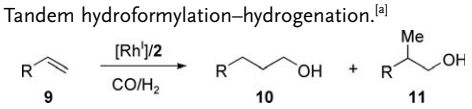

Entry[a]	R	Conversion [%][b]	Yield [%][c]	**10/11**[b]
1	Me	90	87	92:8
2	BzO	95	93	83:17
3	Me, O	100	98	91:9
4	Ph	95	90	7:93

[a] Reaction conditions: $[Rh(CO)_2acac]$/**2**/oct-1-ene (1:10:500), c_0(substrate) = 0.2 M, CH_2Cl_2 (6 mL), 40 °C, CO/H_2 (1:1, 40 bar), 24 h. [b] Substrate conversion and the product ratio were determined by NMR spectroscopy of the crude reaction mixture. [c] Combined yield of the isolated alcohols.

Future studies will address the question as to whether this new reaction mechanism is also applicable to supramolecular substrate activation in other transition-metal-catalyzed reactions.

Received: July 2, 2009
Revised: August 18, 2009
Published online: September 22, 2009

Keywords: aldehydes · homogeneous catalysis · hydroformylation · hydrogenation · rhodium

[1] For reviews on supramolecular catalysis, see: a) *Supramolecular Catalysis* (Ed.: P. W. N. M. van Leeuwen), Wiley-VCH, Weinheim, **2008**; b) B. Breit, *Angew. Chem.* **2005**, *117*, 6976–6986; *Angew. Chem. Int. Ed.* **2005**, *44*, 6816–6825; c) M. J. Wilkinson, P. W. N. M. van Leeuwen, J. N. H. Reek, *Org. Biomol. Chem.* **2005**, *3*, 2371–2383; d) P. A. R. Breuil, F. W. Patureau, J. N. H. Reek, *Angew. Chem.* **2009**, *121*, 2196–2199; *Angew. Chem. Int. Ed.* **2009**, *48*, 2162–2165; e) F. W. Patureau, M. Kuil, J. Sandee, J. N. H. Reek, *Angew. Chem.* **2008**, *120*, 3224–3227; *Angew. Chem. Int. Ed.* **2008**, *47*, 3180–3183; f) L. Yong, F. Yu, H. Yan-Mei, C. Fei, P. Jie, F. Qing-Hua, *Tetrahedron Lett.* **2008**, *49*, 2878–2881.

[2] a) T. Šmejkal, B. Breit, *Angew. Chem.* **2008**, *120*, 317–321; *Angew. Chem. Int. Ed.* **2008**, *47*, 311–315; b) T. Šmejkal, B. Breit, *Angew. Chem.* **2008**, *120*, 4010–4013; *Angew. Chem. Int. Ed.* **2008**, *47*, 3946–3949; c) M. D. Pluth, R. G. Bergman, K. N. Raymond, *Science* **2007**, *316*, 85–88; d) S. Das, C. D. Incarvito, R. H. Crabtree, G. W. Brudvig, *Science* **2006**, *312*, 1941–1943; e) F. Goettmann, P. Le Floch, C. Sanchez, *Chem. Commun.* **2006**, 2036–2038; f) D. B. Grotjahn, *Chem. Eur. J.* **2005**, *11*, 7146–7153; g) J. Yang, B. Gabriele, S. Belvedere, Y. Huang, R. Breslow, *J. Org. Chem.* **2002**, *67*, 5057–5067; h) H. K. A. C. Coolen, J. A. M. Meeuwis, P. W. N. M. van Leeuwen, R. J. M. Nolte, *J. Am. Chem. Soc.* **1995**, *117*, 11906–11913.

[3] K. Weissermel, H.-J. Arpe, *Industrial Organic Chemistry*, Wiley-VCH, Weinheim, **2003**, pp. 127–144.

[4] a) M. C. Simpson, D. J. Cole-Hamilton, *Coord. Chem. Rev.* **1996**, *155*, 163–207; b) R. L. Pruett, *Adv. Organomet. Chem.* **1979**, *17*, 1; c) C. Masters, *Homogeneous Transition-Metal Catalysis: A Gentle Art*, Chapman and Hall, New York, **1981**, and references therein.

[5] a) J. K. MacDougall, M. C. Simpson, M. J. Green, D. J. Cole-Hamilton, *J. Chem. Soc. Dalton Trans.* **1996**, 1161–1172; b) A. J. Sandee, J. N. H. Reek, P. C. J. Kamer, P. W. N. M. van Leeuwen, *J. Am. Chem. Soc.* **2001**, *123*, 8468–8476; c) D. Konya, K. Q. Almeida Leñero, E. Drent, *Organometallics* **2006**, *25*, 3166–3174; d) T. Ichihara, K. Nakano, M. Natayama, K. Nozaki, *Chem. Asian J.* **2008**, *3*, 1722–1728; e) for the hydrogenation of enones under hydroformylation conditions, see: C. J. Scheuermann née Taylor, C. Jaekel, *Adv. Synth. Catal.* **2008**, *350*, 2708–2714.

[6] For reviews of ligand–metal bifunctional catalysis, see: a) R. Noyori, T. Ohkuma, *Angew. Chem.* **2001**, *113*, 40–75; *Angew. Chem. Int. Ed.* **2001**, *40*, 40–73; b) R. Noyori, M. Kitamura, T. Ohkuma, *Proc. Natl. Acad. Sci. USA* **2004**, *101*, 5356–5362; c) S. E. Clapham, A. Hadzovic, R. H. Morris, *Coord. Chem. Rev.* **2004**, *248*, 2201–2237; d) T. Ikariya, K. Murata, R. Noyori, *Org. Biomol. Chem.* **2006**, *4*, 393–406.

[7] For examples of aldehyde hydrogenation, see: a) M. Ito, T. Ikariya, *Chem. Commun.* **2007**, 5134–5142; b) C. P. Casey, S. W. Singer, D. R. Powell, R. K. Hayashi, M. Kavana, *J. Am. Chem. Soc.* **2001**, *123*, 1090–1100; c) M. J. Burk, A. Gerlach, D. Semmeril, *J. Org. Chem.* **2000**, *65*, 8933–8939; d) T. Zweifel, J. V. Naubron, T. Büttner, T. Ott, H. Grützmacher, *Angew. Chem.* **2008**, *120*, 3289–3293; *Angew. Chem. Int. Ed.* **2008**, *47*, 3245–3249; e) C. P. Casey, S. E. Beetner, J. B. Johnson, *J. Am. Chem. Soc.* **2008**, *130*, 2285–2295; f) A. Comas-Vives, G. Ujaque, A. Lledós, *Organometallics* **2007**, *26*, 4135–4144; g) C. P. Casey, J. B. Johnson, *J. Am. Chem. Soc.* **2005**, *127*, 1883–1894; h) C. P. Casey, N. A. Strotman, S. E. Beetner, J. B. Johnson, D. C. Priebe, T. E. Vos, B. Khodavandi, I. A. Guzei, *Organometallics* **2006**, *25*, 1230–1235; i) L. Xu, G. Ou, Y. Yuan, *J. Organomet. Chem.* **2008**, *693*, 3000–3006.

[8] M. S. Taylor, E. N. Jacobsen, *Angew. Chem.* **2006**, *118*, 1550–1573; *Angew. Chem. Int. Ed.* **2006**, *45*, 1520–1543.

[9] For organocatalysis mediated by guanidine, see: a) Y. Sohtome, N. Takemura, K. Takada, R. Takagi, T. Iguchi, K. Nagasawa, *Chem. Asian J.* **2007**, *2*, 1150–1160; b) A. Chuma, H. W. Horn, W. C. Swope, R. C. Pratt, L. Zhang, B. G. G. Lohmeijer, C. C. Wade, R. M. Waymouth, J. L. Hedrick, J. E. Rice, *J. Am. Chem. Soc.* **2008**, *130*, 6749–6754.

[10] a) J. W. Steed, J. L. Atwood, *Supramolecular Chemistry*, Wiley, New York, **2000**; b) C. Schmuck, *Chem. Eur. J.* **2000**, *6*, 709 – 718.

[11] Crystallographic data for **3**: $(C_{18}H_{17}N_4OP)_2(C_4H_8O_2)_2(C_5H_{12})_{0.5}$; colorless crystal of irregular shape, size: $0.20 \times 0.20 \times 0.10\ mm^3$; triclinic, space group $P\bar{1}$, $a = 11.1943(5)$, $b = 11.7553(5)$, $c = 19.4930(5)$ Å, $\alpha = 86.492(2)$, $\beta = 85.938(2)$, $\gamma = 78.8454(16)°$, $V = 2507.47(17)$, $Z = 2$, $\mu = 0.14\ mm^{-1}$; $\lambda = 0.71073$ Å, $T = 293$ K, $2\Theta_{max} = 54.97°$; collected (independent) reflections: 28546 (11455), $R_{int} = 0.0410$, refined parameters (restraints): 612 (25), $R_1 = 0.0687$ for 6600 reflections with $I > 2\sigma$, $wR_2 = 0.2180$ for all data, GOF on $F^2 = 1.024$, max./min. residual electron density: 0.432/−0.268 e Å^3. CCDC 735529 contains the supplementary crystallographic data for this paper. These data can be obtained free of charge from The Cambridge Crystallographic Data Centre via www.ccdc.cam.ac.uk/data_request/cif.

[12] The kinetic data alone do not rule out other interpretations, such as substrate inhibition at higher concentration or coordination of the aldehyde to the rhodium atom prior to hydrogenation.

[13] At the B3LYP/3-21G** level, the energy of the lowest unoccupied Kohn–Sham orbital is lowered by 0.139 au upon hydrogen bonding with the guanidine system. See the Supporting Information for details.

[14] An alternative mechanism for dihydrogen activation, whereby oxidative hydrogen addition to cationic rhodium(I) is followed by proton transfer to the basic guanidine moiety, might also be operative.

[15] The structures were optimized at the B3LYP/6-31G-(d,p)[C,H,N,O,P] + LanL2DZ[Rh] level. Calculations were performed with the software package Gaussian 03 (Revision B.04): M. J. Frisch et al., Gaussian, Inc., Pittsburgh, PA, **2003** (see the Supporting Information).

[16] B. Breit, W. Seiche, *Synthesis* **2001**, 1 – 36.

